Publ. Astron. Obs. Belgrade No. 102 (2022), 113 - 116 *Contributed Paper*

STUDY OF GRAPHENE BY RAINBOW SCATTERING EFFECT

M. HADŽIJOJIĆ[1] and M. ĆOSIĆ[2]

Laboratory of Physics, "Vinča" Institute of Nuclear Sciences
National Institute of the Republic of Serbia, University of Belgrade,
P. O. Box 522, 11001 Belgrade, Serbia
[1]*E-mail milivoje@vin.bg.ac.rs*
[2]*E-mail mcosic@vinca.rs*

Abstract. We have studied transformations of the rainbow pattern generated by the classical rainbow scattering of protons by graphene. Change in the interaction potential transforms rainbow pattern and corresponding angular proton yield. By studying morphological properties of the rainbow pattern it is possible to determine covariance matrix of atomic thermal displacements and characterize point defects present in graphene.

1. DYNAMICS OF PROTON RAINBOW SCATTERING

These are results of proton rainbow transmission through graphene. Selected proton energy is 5 keV. Associated proton de Broglie wavelength of 4.0476×10^{-4} nm is negligible compared to the distance of adjacent carbon atoms. Hence diffraction effects can be neglected and proton trajectories are well approximated by solutions of the classical equations of motion. According to the Ziegler-Biersack-Littmark theory of energy loss, the total proton energy loss and scattering angle dispersion due to interaction with electrons are small compared to the detector resolutions and can be neglected. Probability for neutralization of 5 keV proton is approximately 40%. In calculations we neglected neutralization. Hence calculated and measured angular yields are not comparable unless electrostatic analyzer is implemented to ensure detection of non-neutralized protons only. Let us define the coordinate system such that z-axis coincides with the direction of the proton beam. Direction of the proton beam relative to normal on the crystal surface is specified by polar and azimuthal angles Θ and Φ. Proton–atom interaction potential was constructed by averaging static Doyle–Turner's proton–atom interaction potential over the distribution of thermally induced atom displacements. The covariance matrix of atomic thermal displacements $\mathbf{\Sigma}$ was modeled by Debye theory, and calculated using Molecular Dynamics approach. More realistic model of graphene thermal motion was constructed using Molecular Dynamics. Let

(v_x, v_y, v_z) be the velocity of the transmitted proton. Proton scattering angles θ_x and θ_y are defined by expressions:

$$\tan\theta_x = \frac{v_x}{v_z}, \quad \tan\theta_y = \frac{v_y}{v_z}. \tag{1}$$

Angular yield of transmitted protons $Y(\theta_x, \theta_y)$ is the number of protons scattered in the element $d\theta_x d\theta_y$ centered at the (θ_x, θ_y). Proton impact parameter (b_x, b_y) is projection of the proton initial position to the (x, y) plane. Proton trajectories define mapping of the proton impact parameters to the set of proton scattering angles:

$$f_{(\Theta,\Phi)}: (b_x, b_y) \rightarrow (\theta_x, \theta_y), \tag{2}$$

where Θ and Φ are parameters. Differential cross section is given by the expression:

$$\sigma(b_x, b_y; \Theta, \Phi) \sim \left|\det \mathcal{J}_{(\theta_x,\theta_y)}(b_x, b_y)\right|^{-1}, \tag{3}$$

where $\mathcal{J}_{(\theta_x,\theta_y)}(b_x, b_y)$ is Jacobian matrix of the mapping (2). σ is infinite if Jacobian matrix is singular. Singularities of $\mathcal{J}_{(\theta_x,\theta_y)}(b_x, b_y)$ are curves in the impact parameter plane. Images of these curves obtained by mapping (2) are *rainbow lines*. As singularities of differential cross section, rainbow lines have significant influence on shape of the angular distribution of transmitted protons. Optical rainbow, nuclear, Coulomb and crystal rainbow effects are manifestations of the same rainbow scattering effect. Next will be shown how study of the rainbow pattern could be utilized for characterization of graphene.

2. CHARACTERIZATION OF GRAPHENE

We have investigated influence of covariance matrix **Σ** and graphene defects on the angular distributions and associated rainbow patterns of transmitted protons. Three different cases were analyzed: perfect graphene with atoms performing isotropic oscillations, perfect graphene with atoms performing anisotropic oscillations, and graphene with vacancies and isotropic thermal motion of atoms. Figures 1(a)-1(c) are illustrations of these three cases. In the case of isotropic atomic displacements, **Σ** is a scalar matrix and interaction potential near individual atoms has a spherical symmetry. This is not the case if atomic thermal vibrations are anisotropic. Blue surfaces represent equipotential surfaces in the vicinity of the individual carbon atoms. In figures 1(a')-1(c') are shown corresponding angular distributions of transmitted protons, calculated by solving equations of motion. Angular yields are presented in the scattering angle plane (θ_x, θ_y). Maximal scattering angles are approximately 150 mrad. Rectangular insets 1(a")-1(c") are enlarged views of the angular distributions in the regions of small scattering angles. Black curves are

calculated rainbow lines. Particle count is large along rainbow lines and they outline shapes of all angular distributions. The outer rainbows O_1, O_2 and O_3 are formed by protons which experienced close collisions with carbon atoms. Hence outer rainbows contain information about properties of the interaction potential in the vicinity of individual atoms. Consequently outer rainbow O_1 is circular regardless of direction of the incident proton beam. In figures 1(b') and 1(b") are shown angular yields and rainbow patterns of protons transmitted through graphene with anisotropic thermal vibrations of carbon atoms. In this case interaction potential near individual atoms does not have a spherical symmetry. Hence shape of the outer part of angular distribution is not necessarily circular. In general, corresponding outer rainbow O_2, and consequently the entire distribution, has shape of a tilted ellipse. Symmetry axes of rainbow O_2 are represented by cyan lines.

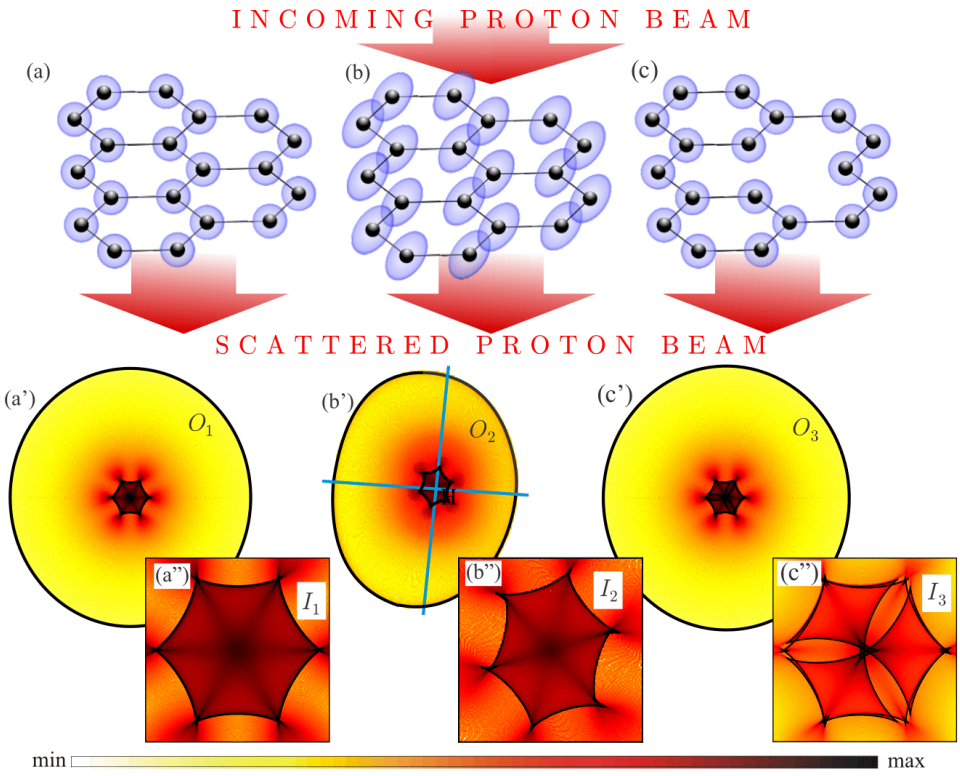

Figure 1: (a),(b) Illustrations of perfect graphene in the case of isotropic and anisotropic atomic thermal vibrations; (c) graphene with vacancies and isotropic thermal motion of atoms. Blue surfaces are sketches of equipotential surfaces near carbon atoms. (a')-(c') corresponding angular yields, color-coded according to the color bar. Rectangular insets (a")-(c") are enlarged views of angular distributions in the range of small scattering angles. Rainbows are shown by black lines. Cyan lines are symmetry axes of the rainbow O_2.

Outer rainbow line O_3 in figure 1(c') is indistinguishable from the rainbow O_1. This is consequence of the isotropic thermal vibrations of carbon atoms. We found that outer rainbow line behaves qualitatively equal as normal projection of the ellipsoid associated with the matrix $\mathbf{\Sigma}^{-1}$. We showed that parameters of the outer rainbow line could be used to solve the inverse problem, i.e. to determine the covariance matrix $\mathbf{\Sigma}$, even if atoms perform anisotropic and correlated motion. The inner rainbow lines, labeled by I_1, I_2 and I_3, are generated by synergetic action of carbon atoms forming graphene lattice. Therefore, inner rainbow pattern carries information about crystal structure. Symmetry of the inner rainbows I_1 and I_2 coincides with the symmetry of the graphene hexagon projected to the (x, y) plane. We showed that inner rainbows are not influenced by the thermal motion of carbon atoms. The inner rainbow pattern I_3 is generated by protons transmitted through graphene with vacancies. It is composed of four rainbow lines. It differs significantly from the inner rainbow pattern formed by proton scattering on a perfect graphene. We found that different defect types produce different inner rainbow patterns. Furthermore, we have shown that rainbow patterns and angular distributions of protons transmitted through graphene with point defects could be used to determine densities of the unknown defects even in the case of a sample containing a combination of the different defect types. Developed procedure could enable characterization of graphene defects.

References

Adams, A. : 2002, *Phys. Rep.* **356**, 229.
Connor, J. N. L., Farrelly, D. : 1981, *J. Chem. Phys.* **75**, 2831.
Ford K. W., Wheeler, J. A. : 2002 (reprinted), *Ann. Phys.* **281**, 608.
Gruber, E., et al, : 2016, *Nat. Commun.* 7, 1-7 (Supplementary material).
Nešković, N. : 1986, *Phys. Rev. B* **33**, 6030.
Zhao, S. et al, : 2016, *J. Phys. Condens. Matter* 27, 1-6.
Ćosić, M., Hadžijojić, M., Petrović, S., Rymzhanov, R., Bellucci, S. : 2019, *Carbon* **145**, 161.
Ćosić, M., Hadžijojić, M., Petrović, S., Rymzhanov, R. : 2021, *Chaos* **31**, 093115.
Hadžijojić, M., Ćosić, M., Rymzhanov, R. : 2021, *J. Phys. Chem. C*. **125**, 38, 21030–21043.